

DTIC COPY

4

REPORT SD-TR-88-90

AD-A200 463

# Use of Rutherford Backscattering and Optical Spectroscopy to Study Boron Implantation in Cadmium Telluride

D. N. JAMIESON  
California Institute of Technology  
Pasadena, CA 91115

R. C. BOWMAN, JR.  
Chemistry and Physics Laboratory

P. M. ADAMS  
Materials Sciences Laboratory

and

J. F. KNUDSEN  
Electronics Research Laboratory  
Laboratory Operations  
The Aerospace Corporation  
El Segundo, CA 90245

and

R. G. DOWNING  
National Bureau of Standards  
Gaithersburg, MD 20899

3 October 1988

Prepared for  
SPACE DIVISION  
AIR FORCE SYSTEMS COMMAND  
Los Angeles Air Force Base  
P.O. Box 92960  
Los Angeles, CA 90009-2960

DTIC  
ELECTE  
OCT 28 1988  
S  
D  
OE  
E

APPROVED FOR PUBLIC RELEASE:  
DISTRIBUTION UNLIMITED


88 10 27 0

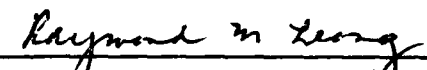
This report was submitted by The Aerospace Corporation, El Segundo, CA 90245, under Contract No. F04701-85-C-0086 with the Space Division, P.O. Box 92960, Worldway Postal Center, Los Angeles, CA 90009-2960. It was reviewed and approved for The Aerospace Corporation by S. Feuerstein, Director, Chemistry and Physics Laboratory.

Lt Constance M. Chintall/CNCIV was the project officer for the Mission-Oriented Investigation and Experimentation (MOIE) Program.

This report has been reviewed by the Public Affairs Office (PAS) and is releasable to the National Technical Information Service (NTIS). At NTIS, it will be available to the general public, including foreign nationals.

This technical report has been reviewed and is approved for publication. Publication of this report does not constitute Air Force approval of the report's findings or conclusions. It is published only for the exchange and stimulation of ideas.

  
for CONSTANCE M. CHINTALL, Lt, USAF  
MOIE Project Officer  
SD/CNCIV

  
RAYMOND M. LEONG, Maj, USAF  
Deputy Director, AFSTC West Coast Office  
AFSTC/WCO OL-AB

UNCLASSIFIED

SECURITY CLASSIFICATION OF THIS PAGE

## REPORT DOCUMENTATION PAGE

1a. REPORT SECURITY CLASSIFICATION Unclassified			1b. RESTRICTIVE MARKINGS		
2a. SECURITY CLASSIFICATION AUTHORITY			3. DISTRIBUTION / AVAILABILITY OF REPORT Approved for public release; distribution unlimited.		
2b. DECLASSIFICATION / DOWNGRADING SCHEDULE					
4. PERFORMING ORGANIZATION REPORT NUMBER(S) TR-0088(3945-07)-2			5. MONITORING ORGANIZATION REPORT NUMBER(S) SD-TR-88-90		
6a. NAME OF PERFORMING ORGANIZATION The Aerospace Corporation Laboratory Operations		6b. OFFICE SYMBOL (If applicable)		7a. NAME OF MONITORING ORGANIZATION Space Division	
6c. ADDRESS (City, State, and ZIP Code) El Segundo, CA 90245			7b. ADDRESS (City, State, and ZIP Code) Los Angeles Air Force Base Los Angeles, CA 90009-2960		
8a. NAME OF FUNDING / SPONSORING ORGANIZATION		8b. OFFICE SYMBOL (If applicable)		9. PROCUREMENT INSTRUMENT IDENTIFICATION NUMBER F04701-85-C-0086-P00019	
8c. ADDRESS (City, State, and ZIP Code)			10. SOURCE OF FUNDING NUMBERS		
			PROGRAM ELEMENT NO.	PROJECT NO.	TASK NO.
			WORK UNIT ACCESSION NO.		
11. TITLE (Include Security Classification) Use of Rutherford Backscattering and Optical Spectroscopy to Study Boron Implantation on Cadmium Telluride					
12. PERSONAL AUTHOR(S) Jamieson, D. N. (Calif. Inst. of Tech.); Bowman, R. C., Jr., Adams, P. M., Knudsen, J. F. (The Aerospace Corporation); and Downing, R. G. (National Bureau of Standards)					
13a. TYPE OF REPORT		13b. TIME COVERED FROM TO		14. DATE OF REPORT (Year, Month, Day) 1988 October 3	
				15. PAGE COUNT 19	
16. SUPPLEMENTARY NOTATION					
17. COSATI CODES			18. SUBJECT TERMS (Continue on reverse if necessary and identify by block number)		
FIELD	GROUP	SUB-GROUP	Optical detectors		
			Electromodulation spectroscopy		
19. ABSTRACT (Continue on reverse if necessary and identify by block number)					
<p>The effect of large dose boron implantation in single crystal cadmium telluride (CdTe) has been investigated by Rutherford backscattering spectrometry (RBS), with channeling double crystal x-ray diffraction (DCD), and photoreflectance (PR) spectroscopy. Comparisons are made with the results of identical B implantations of Si and GaAs crystals. Multiple energy implantations were performed at room temperature and liquid nitrogen temperature with total doses up to <math>1.5 \times 10^{16}</math> B<sup>+</sup> ions/cm<sup>2</sup>. The implanted B distribution was measured with neutron depth profiling (NDP) and found to agree well with Monte Carlo ion range calculations. The RBS results showed that the CdTe crystals had not been rendered completely amorphous even for the highest dose implantation unlike GaAs and Si. Furthermore, the DCD results showed little implantation-induced structure in the rocking curves from the implanted CdTe crystals, in contrast to GaAs. The consequences of annealing at 500°C in an attempt to regrow the crystal structure are also discussed.</p>					
20. DISTRIBUTION / AVAILABILITY OF ABSTRACT <input checked="" type="checkbox"/> UNCLASSIFIED/UNLIMITED <input type="checkbox"/> SAME AS RPT. <input type="checkbox"/> DTIC USERS				21. ABSTRACT SECURITY CLASSIFICATION Unclassified	
22a. NAME OF RESPONSIBLE INDIVIDUAL				22b. TELEPHONE (Include Area Code)	
				22c. OFFICE SYMBOL	

# PREFACE

The assistance of R. L. Alt, G. Bai, and R. E. Robertson with some of the measurements is greatly appreciated. D. N. Jamieson acknowledges support at Caltech by NSF grant No. DMR-8421119, as well as by the Semiconductor Research Corporation under contract No. 87-SJ-100.

<b>Accession For</b>	
NTIS GRA&I	<input checked="" type="checkbox"/>
DTIC TAB	<input type="checkbox"/>
Unannounced	<input type="checkbox"/>
Justification	
By _____	
Distribution/	
Availability Codes	
Dist	Avail and/or Special
A-1	

## CONTENTS

I.	INTRODUCTION.....	5
II.	EXPERIMENT.....	7
III.	RESULTS.....	9
IV.	DISCUSSION.....	15
V.	CONCLUSIONS.....	19
	REFERENCES.....	21

## FIGURES

1.	Comparison of Normalized RBS Channeling Spectra Obtained for (a) Unimplanted $\langle 100 \rangle$ CdTe, $\langle 100 \rangle$ GaAs, $\langle 100 \rangle$ Si, (b) Narrow RT, (c) Narrow LN2, and (d) Deep RT Implantations.....	10
2.	DCD X-Ray Rocking Curves; the Upper Curve in Each Pair is for CdTe, the Lower for GaAs: (a) Unimplanted, (b) Narrow RT, (c) Narrow LN2 and (d) Deep RT Implantations.....	12
3.	PR Lineshapes for (a) Unimplanted CdTe, (b) Narrow RT, and (c) Narrow RT followed by 500°C, 1 h Anneal.....	13
4.	Effective Displaced Atom Concentrations Obtained from the Channeling Spectra (see text) (b) Narrow RT, (c) Narrow LN2, (d) Deep RT, (a) Shows the B Profile Measured by NDP Compared to a TRIM Calculation.....	16

## 1. INTRODUCTION

The II-VI compound cadmium telluride (CdTe) has properties that make it useful for applications in several areas. With a direct band gap of 1.5 eV, it is useful as an optical detector. In addition, CdTe is used as a substrate for the ternary compound  $\text{Hg}_{(1-x)}\text{Cd}_x\text{Te}$  to fabricate detectors for infrared radiation.<sup>1</sup> CdTe crystals have also been used as high resolution room temperature x-ray and gamma ray detectors of relatively high efficiency compared to Si or Ge because of a relatively large average electron density.<sup>2,3</sup> Recently, a novel application of large area CdTe gamma ray detectors has been proposed to search for events from double-beta decay candidates  $^{114}\text{Cd}$ ,  $^{116}\text{Cd}$ ,  $^{128}\text{Te}$ , and  $^{130}\text{Te}$ . Fabrication of a CdTe FET device has been reported<sup>4</sup> with the possibility of monolithic integration of detectors and devices.

Ion implantation could play a role in CdTe device fabrication, however, Sigmon<sup>1</sup> points out that although the effects of ion implantation in elemental and III-V compound semiconductors are relatively well understood, this is not the case for II-VI compounds. The present work shows that the effect of B implantation into CdTe is quite different compared to Si and GaAs. B was used because of its potential use as a dopant in  $\text{Hg}_{(1-x)}\text{Cd}_x\text{Te}$ . Comparisons are also made to theoretical results from the Monte Carlo computer code TRIM.<sup>5</sup>

## 11. EXPERIMENT

Three multiple-energy B implantations were done into randomly oriented single crystal CdTe samples. The experimental parameters of the three implantations are listed in Table 1. The three implantations will be referred to as 'narrow RT,' 'narrow LN2' and 'deep RT', where RT (nominally 293 K) and LN2 (nominally 77 K) refer to the sample temperature during the implantations. Identical implantations were also done into GaAs and Si crystals. In all cases, the implantation current was kept below  $0.25 \mu\text{A}/\text{cm}^2$  to minimize effects from sample heating. The narrow RT implantation was done with  $^{10}\text{B}$  so that the B distribution could be measured with neutron depth profiling<sup>6</sup> by the reaction  $^{10}\text{B}(n, \alpha)^7\text{Li}$ .

Table 1. B Implant Conditions

Implant name	Ion	Ion Energies (keV)	Implant Temperature (K)	B Dose ( $10^{15}/\text{cm}^2$ )	Total B Dose ( $10^{10}/\text{cm}^2$ )
Narrow RT	$^{10}\text{B}^+$	50	293	5	15
		100		10	
Narrow LN2	$^{11}\text{B}^+$	50	77	5	10
		100		5	
Deep RT	$^{11}\text{B}^+$	40	293	1	3
		100		1	
		400		1	

Following the implantations, the strain was measured from rocking curves<sup>7</sup> obtained with a double crystal x-ray diffractometer. In this case,  $\text{Cu K}_{\alpha 1}$  radiation from (400) reflections from a Ge monochromator crystal was used to obtain the rocking curves from (400) reflections in the samples.

RBS channeling measurements were subsequently performed with a 2 MeV  $\text{He}^+$  beam and a scattering angle of  $170^\circ$ . During the procedures for alignment of the crystal  $\langle 100 \rangle$  axes with the incident beam and the time required to collect the spectra, the crystals received a total dose of up to  $3 \times 10^{16} \text{ He}^+/\text{cm}^2$ . Significant changes were observed in rocking curves obtained after the channeling measurements in GaAs; hence, fresh places on all samples were selected for analyses performed after RBS measurements.

Attempts were made to anneal out the ion implantation damage by annealing at  $500^\circ\text{C}$ , which has previously been reported to largely remove damage in CdTe generated by Bi implantation;<sup>8</sup> however, the duration used in this anneal was not stated. RBS results from the present samples suggested that very little improvement occurred after annealing at  $500^\circ\text{C}$  for 1 hour, except possibly at the surface. Photorefectance (PR) measurements were made to investigate the crystal quality after the anneal.



### III. RESULTS

RBS channeling spectra for unimplanted CdTe, GaAs, and Si crystals are shown in Fig. 1a. The depth scales for the RBS spectra have been calculated following the numerical procedure outlined by Chu et al.<sup>9</sup> The true atom densities of the crystals (for Si:  $N=4.99$ , GaAs:  $N=4.428$ , and CdTe:  $N=2.94 \times 10^{22}$  atom/cm<sup>3</sup>) were used in the calculation; however, the stopping cross-section factor,  $[s]$ , and the scattering cross section,  $\sigma$ , of the GaAs and CdTe crystals were calculated as if they were composed of As and Te, respectively. The small offset between the depth scales for the elements in the compounds is neglected. The spectrum heights have been normalized to the randomly oriented CdTe spectrum height to compensate for the differing scattering cross sections of the various elements. The results for the unimplanted crystals show an  $X_{\min}$  (the ratio of the yield for the aligned crystal to that of the randomly aligned crystal) of 2.1%, 4.7%, and 10% for  $\langle 100 \rangle$  Si,  $\langle 100 \rangle$  GaAs, and  $\langle 100 \rangle$  CdTe, respectively. These values show that the unimplanted CdTe is not as high quality as some CdTe crystals reported in the literature;<sup>8</sup> however, this was not important since the B implantations produce damage that was readily observable compared to the defects already present in the starting material.

The effect of the narrow RT implant on CdTe was to apparently make the crystal almost amorphous (Fig. 1b), with the  $X_{\min}$  rising to 82% at the depth which produces the greatest backscattering yield. This is very much greater than for GaAs (47%) or Si (39%). The yield is greater in CdTe partly because of the larger scattering cross section from the heavier atoms in this crystal that will enhance dechanneling.

Following the narrow LN<sub>2</sub> implantation (Fig. 1c), the Si and GaAs crystals were apparently made amorphous ( $X_{\min} = 100\%$ ); however, the  $X_{\min}$  in CdTe rose to 80%, which was approximately the same as the narrow RT implant. CdTe was therefore more difficult to make completely amorphous compared to Si or GaAs but may nevertheless be easily damaged. This could

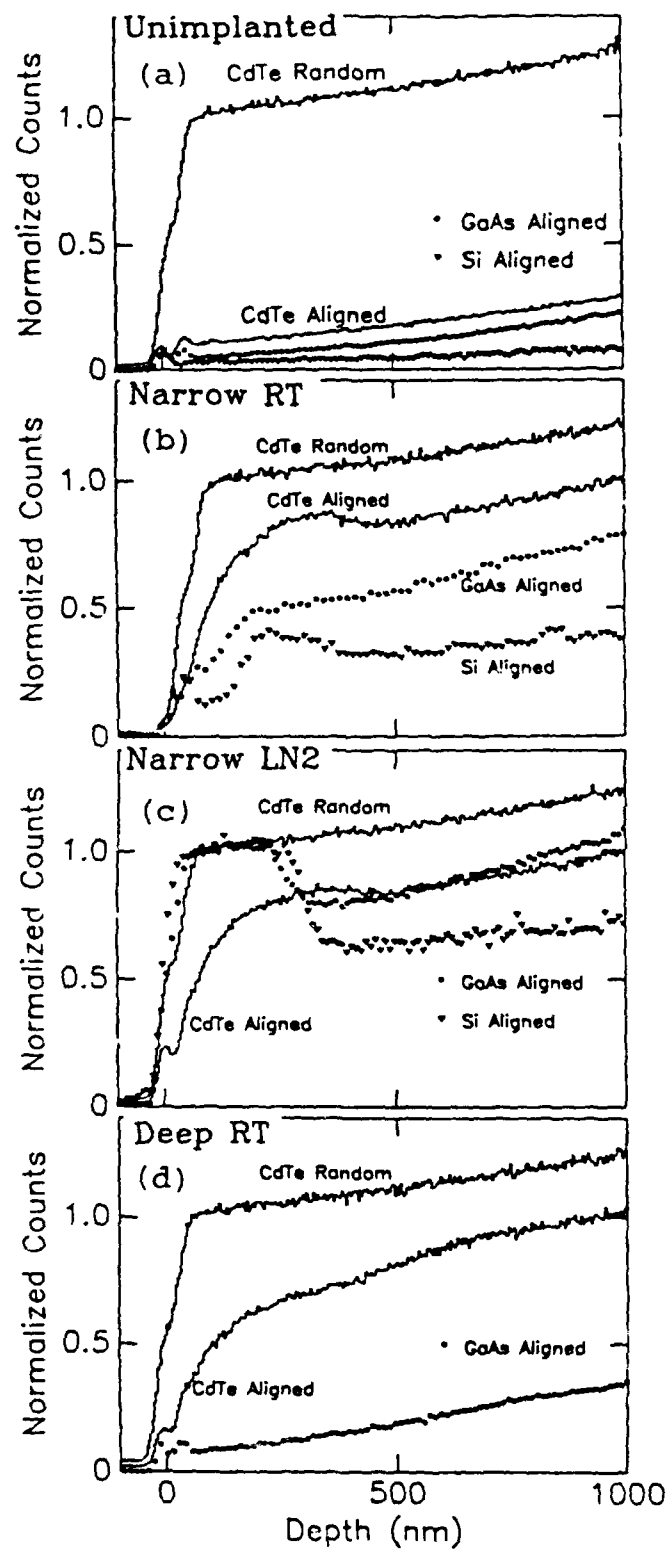


Fig. 1. Comparison of Normalized RBS Channeling Spectra Obtained for: (a) Unimplanted  $\langle 100 \rangle$  CdTe,  $\langle 100 \rangle$  GaAs,  $\langle 100 \rangle$  Si, (b) Narrow RT, (c) Narrow LN2, and (d) Deep RT Implantations.

also be seen in the deep RT implantation (Fig. 1d). Here the total dose was one-fifth that used in the narrow implantations, and this was reflected by the fact that very little damage is evident in the GaAs spectrum. However, the CdTe was again severely damaged ( $X_{\min} > 66\%$ ).

Normalized x-ray rocking curves obtained from the unimplanted GaAs and CdTe crystals, as well as curves obtained after the three implantations, are compared in Fig. 2. Structure appears in the rocking curves for the implanted GaAs contributed by implantation-induced strain in the crystal that has caused an expansion of the GaAs crystal planes normal to the surface.<sup>10</sup> No comparable structure appears for CdTe, out to  $|\Delta\theta| = 0.18^\circ$ , except for a single satellite peak seen in the deep RT sample. This satellite peak implies that the implant has produced a layer of average strain of 0.07%, which is an order of magnitude smaller than the strains seen in GaAs. It is possible that satellite peaks are also present in the spectra for the other CdTe samples but were not resolved from the main peak. However, it can be concluded that the implantations in CdTe generally produce buried strained layers with considerably smaller strain compared to those seen in GaAs.<sup>10</sup>

Several optical properties of CdTe have been shown to be altered by B implantations.<sup>11-13</sup> However, most optical methods can probe less than 100 nm from the surface, which is shallow compared to the damage produced by the present implants. PR measurements were found useful for investigation of the effects of annealing the narrow RT sample. PR is a contactless version of electromodulation spectroscopy<sup>14</sup> for measurement<sup>12</sup> of the band gap optical transition energy. Results, obtained at room temperature, are shown in Fig. 3. The PR lineshapes have been fitted with a standard Aspnes function,<sup>15</sup> which enabled the empirical linewidth parameter,  $\Gamma$ , to be determined. The linewidth for the unimplanted material was found to be 24 meV. After the narrow RT implantation, the resulting linewidth has broadened significantly and reduced in amplitude, showing that severe disorder had been introduced into the crystal as also seen from RBS results (not shown). The PR lineshape in this case could not be well

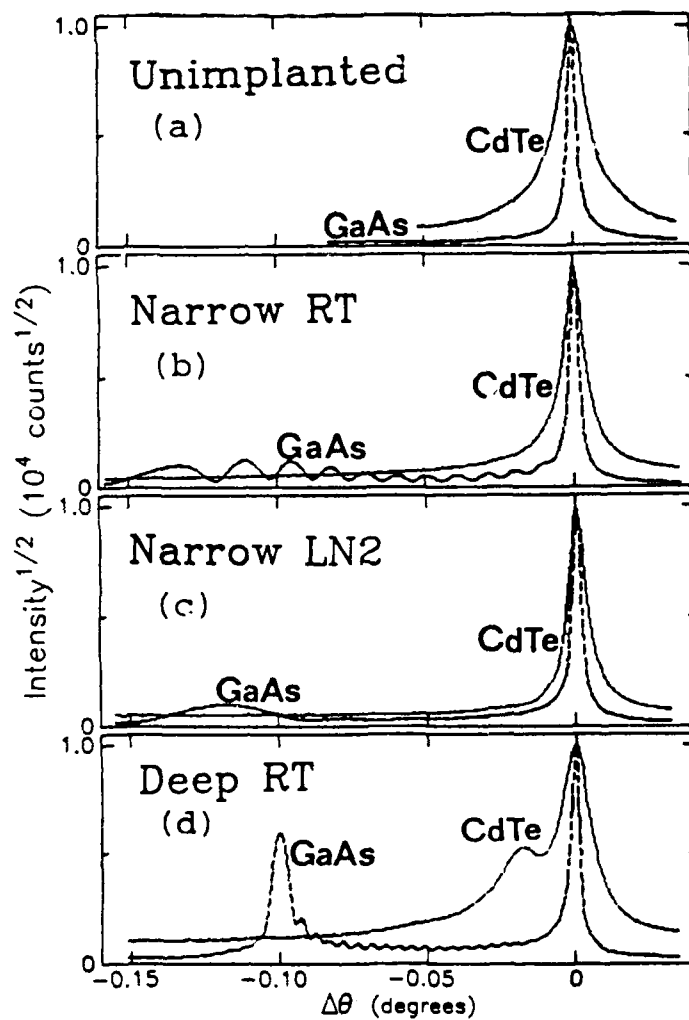


Fig. 2. DCD X-ray Rocking Curves. The Upper Curve in Each Pair is for CdTe, the Lower for GaAs: (a) Unimplanted, (b) Narrow RT, (c) Narrow LN2, and (d) Deep RT Implantations.

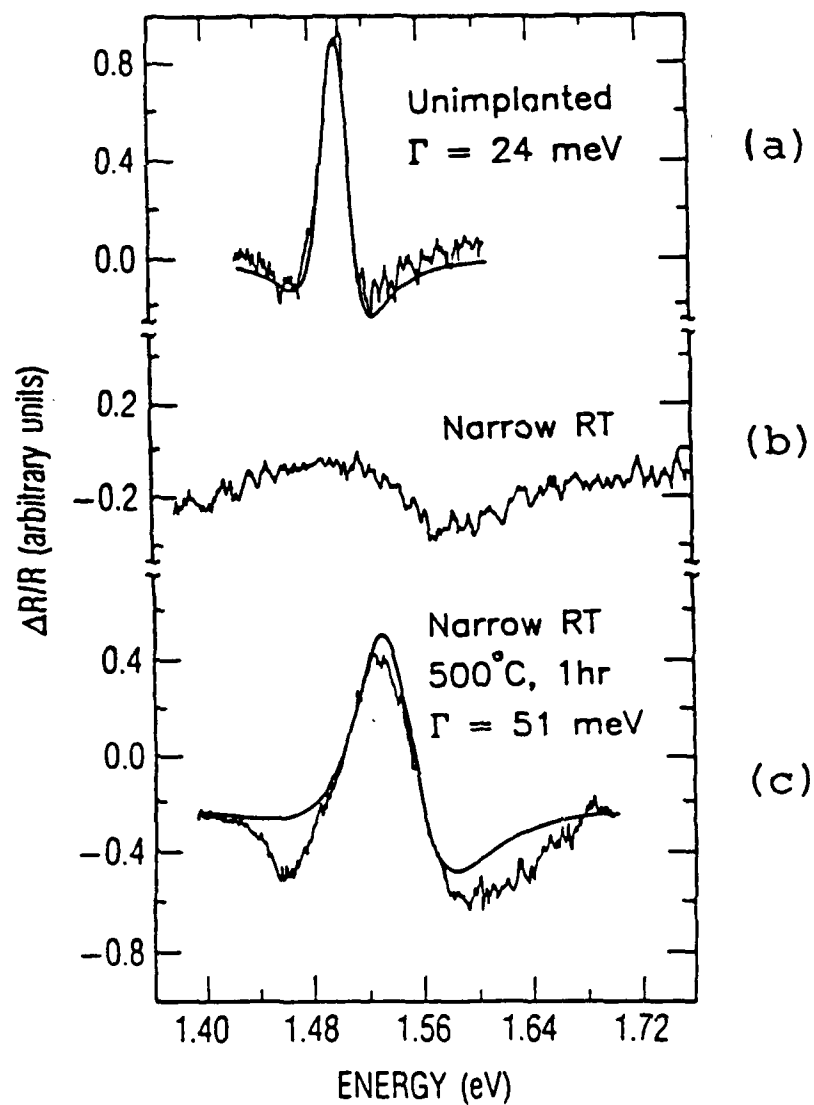


Fig. 3: PR Lineshapes for (a) Unimplanted CdTe, (b) Narrow RT, and (c) Narrow RT Followed by 500°C, 1 h Anneal.

fitted with the Aspnes function. After annealing the sample at 500°C for 1 h, the lineshape recovered some of the amplitude and had width of 51 meV, more than twice as wide as the unimplanted material. Similar results were obtained from other CdTe samples with different implantation conditions.<sup>12</sup> These results suggest that some of the disorder produced by the B implantation could be reduced by the 500°C anneal for 1 h; however, the increased PR linewidth and the RBS results show that significant residual damage is still present.

#### IV. DISCUSSION

It is not possible to quantitatively compare the damage produced in the crystals by direct comparison of the RBS spectra for the aligned, implanted crystals because the yields are the sum of a peak contributed by direct scattering from defects and an error-function-like yield contributed by cumulative dechanneling by the defects.<sup>16</sup> The contribution from dechanneling was modeled by a linear function,<sup>17</sup> which was subtracted from the raw spectra of the implanted crystals (Fig. 1b, c, d) to give the direct scattered fraction. The direct scattered fraction was numerically converted into the displaced atom density by assuming that the direct scattering factor<sup>16</sup> was equal to unity. This assumption is true if all of the scattering centers are isolated displaced atoms. Since the formation of extended defects cannot be ruled out, the result is termed the "effective displaced atom density," hereafter referred to as "EDAD."

Given the approximations involved here, this is a zeroth order representation of the damage profile in CdTe. The approximations are less severe when the same procedure is applied to Si and GaAs because of the smaller contribution to the backscattered yield from the dechanneled fraction. So that the results for the three different crystals could be compared, the EDAD was divided by the atomic densities to give the percentage of displaced atoms. The results are shown in Fig. 4. The maximum EDAD for CdTe is close to 40% for each implantation, despite wide variations for GaAs (<5% to 100%) and for Si (25% to 100%). This implies that the damage in CdTe is not a strong function of the implantation parameters when the B dose is above  $3 \times 10^{15}$  B/cm<sup>2</sup>, in agreement with previous results for Bi, Te, and In implantation where the damage was found to increase with the log of the dose.<sup>8</sup> The damage profile in CdTe appears to be correlated with the number of displacements per atom (dpa) calculated from the modified Kinchin-Pease relation:<sup>18</sup>

$$\text{dpa}(x) = \frac{0.4}{N E_d} \frac{dE}{dx} D \quad (1)$$

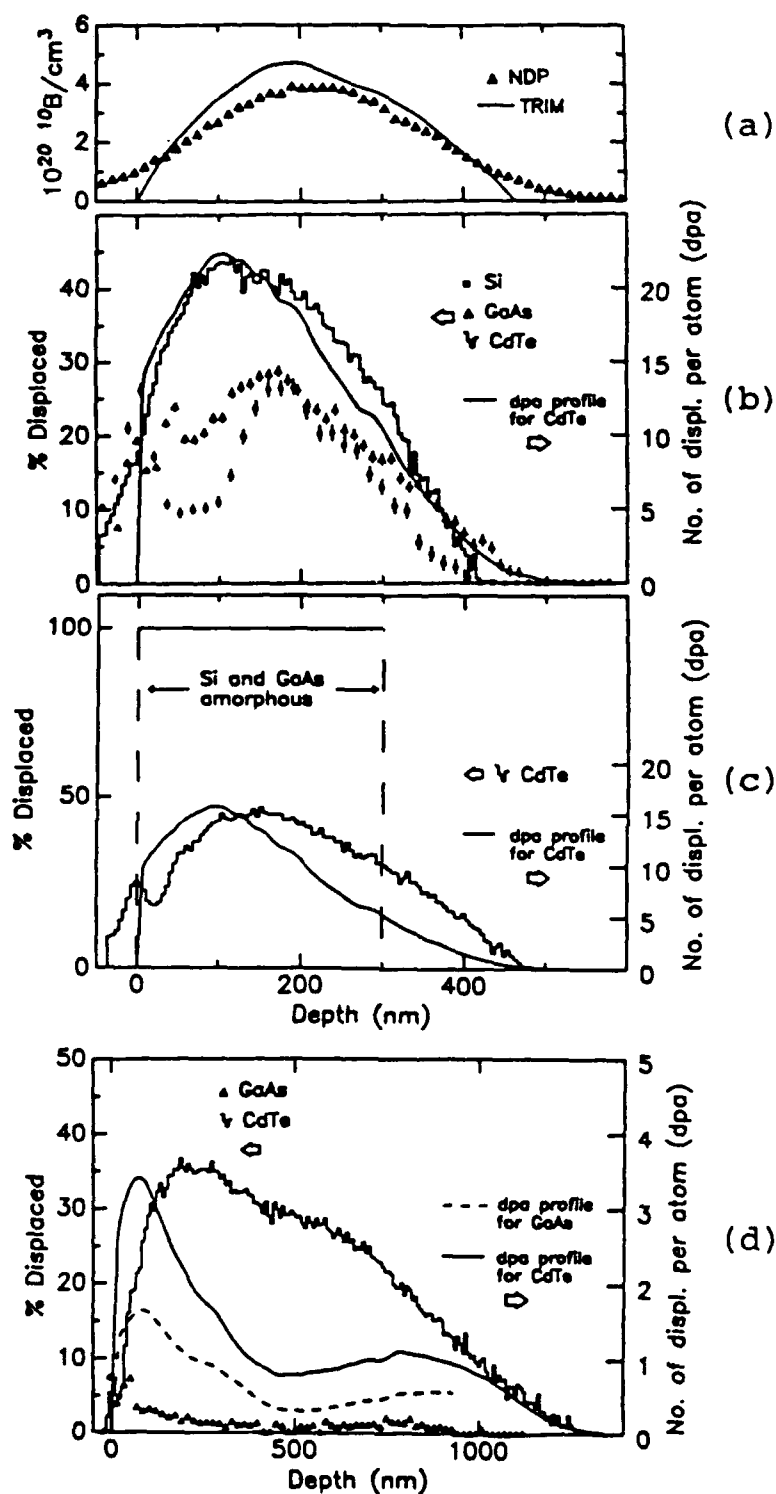


Fig. 4. Effective Displaced Atom Concentrations Obtained from the Channeling Spectra (see text), (b) narrow RT, (c) narrow LN2, (d) deep RT. (a) Shows the B profile Measured by NDP Compared to a TRIM Calculation.



where  $E_d$  is the average displacement energy of the Cd and Te lattices equal to 6.7 eV,<sup>8</sup>  $dE/dx$  is the damage energy density per ion from the computer program TRIM<sup>6</sup>, and  $D$  is the B ion dose. The results show that the centroid of the effective displaced atom concentration coincides closely with the peak in the dpa profile (Fig. 4b, c, d) as well as the peak in the B concentration profile from the NDP measurement (Fig. 4a).

## V. CONCLUSIONS

CdTe behaves quite differently upon B implantation compared to Si and GaAs. The small displacement energy of the CdTe lattice (6.7 eV, Ref. 8) compared to GaAs (9 eV, Ref. 19) and Si (14 eV, Ref. 20) probably accounts for the relative ease with which CdTe may be damaged. The polarity parameter<sup>21</sup> of the CdTe lattice (0.78) suggests that the difficulty of amorphization is because of the more ionic nature of CdTe compared to GaAs (0.47) and Si (0). The polarity parameter is zero for non-polar lattices and 1 for completely polar lattices. Further, the nature of the defects induced in CdTe by the implantation do not give rise so readily to strained layers compared to GaAs.

## REFERENCES

1. T. W. Sigmon, Nucl. Instrum. Methods, in Phys. Res. B7/8, 402 (1985).
2. E. Sakai, Nucl. Instrum. Methods, 196, 121 (1982).
3. T. Hazlett, H. Cole, M. R. Squillante, G. Entine, G. Sugars, W. Fecych, and O. Tench, IEEE Trans. on Nucl. Sci., 33, 332 (1986).
4. D. L. Dreifus, R. M. Kilbas, K. A. Harris, R. N. Bicknell, R. L. Harper, and J. F. Schetzina, Appl. Phys. Lett., 51 (12), 931 (1987).
5. J. P. Biersack, Nucl. Instr. Meth. in Phys. Res., B27, 21 (1987).
6. R. G. Downing, R. F. Fleming, J. K. Langland, and D. H. Vincent, Nucl. Instrum. Methods, 218, 47 (1983).
7. V. S. Speriosu, B. M. Paine, M-A. Nicolet, and H. L. Glass, Appl. Phys. Lett., 40, 604 (1982).
8. M. Gettings and K. G. Stephens, Rad. Effects, 22, 53 (1974).
9. W. K. Chu, J. W. Mayer, and M-A. Nicolet, Backscattering Spectrometer, (Academic Press, 1978).
10. G. Bai, D. N. Jamieson, M-A. Nicolet, and T. Vreeland Jr. in Materials Modification and Growth Using Ion Beams, edited by U. J. Gibson, A. E. White, and P. P. Pronko (Mater. Res., Soc. Proc. 93, Pittsburgh, PA 1986) pp. 67-72.
11. K. M. James, J. L. Merz, and C. E. Jones, J. Appl. Phys., 60, 3699 (1986).
12. R. C. Bowman, Jr., R. C. Alt, P. M. Adams, J. F. Knudsen, D. N. Jamieson, and R. G. Downing, J. Cryst. Growth, 86, 768 (1988).
13. R. C. Bowman, Jr. and D. N. Jamieson, Proc. SPIE Symp., 822, 31 (1987).
14. F. H. Pollak, Proc. SPIE Symp., 276, 142 (1981).
15. D. E. Aspnes, Surf. Sci., 37, 418 (1973).
16. L. C. Feldman, J. W. Mayer, S. T. Picraux, Materials Analysis by Ion Channeling (Academic Press, 1982).

17. F. H. Eisen in Channeling, edited by D. V. Morgan (Wiley, 1973), pp. 415-434.
18. G. H. Kinchin and R. S. Pease, Rep. Prog. Phys., 18, 1 (1955).
19. D. Pons and J. Bourgoïn, Phys. Rev. Lett., 47 (18), 1293 (1981).
20. H. H. Anderson, Appl. Phys. Lett., 18, 131 (1979).
21. W. A. Harrison, Electronic Structure and the Properties of Solids (W. H. Freeman and Co., 1980).

## LABORATORY OPERATIONS

The Aerospace Corporation functions as an "architect-engineer" for national security projects, specializing in advanced military space systems. Providing research support, the corporation's Laboratory Operations conducts experimental and theoretical investigations that focus on the application of scientific and technical advances to such systems. Vital to the success of these investigations is the technical staff's wide-ranging expertise and its ability to stay current with new developments. This expertise is enhanced by a research program aimed at dealing with the many problems associated with rapidly evolving space systems. Contributing their capabilities to the research effort are these individual laboratories:

Aerophysics Laboratory: Launch vehicle and reentry fluid mechanics, heat transfer and flight dynamics; chemical and electric propulsion, propellant chemistry, chemical dynamics, environmental chemistry, trace detection; spacecraft structural mechanics, contamination, thermal and structural control; high temperature thermomechanics, gas kinetics and radiation; cw and pulsed chemical and excimer laser development including chemical kinetics, spectroscopy, optical resonators, beam control, atmospheric propagation, laser effects and countermeasures.

Chemistry and Physics Laboratory: Atmospheric chemical reactions, atmospheric optics, light scattering, state-specific chemical reactions and radiative signatures of missile plumes, sensor out-of-field-of-view rejection, applied laser spectroscopy, laser chemistry, laser optoelectronics, solar cell physics, battery electrochemistry, space vacuum and radiation effects on materials, lubrication and surface phenomena, thermionic emission, photo-sensitive materials and detectors, atomic frequency standards, and environmental chemistry.

Computer Science Laboratory: Program verification, program translation, performance-sensitive system design, distributed architectures for spaceborne computers, fault tolerant computer systems, artificial intelligence, micro-electronics applications, communication protocols, and computer security.

Electronics Research Laboratory: Microelectronics, solid-state device physics, compound semiconductors, radiation hardening; electro-optics, quantum electronics, solid-state lasers, optical propagation and communications; microwave semiconductor devices, microwave/millimeter wave measurements, diagnostics and radiometry, microwave/millimeter wave thermionic devices; atomic time and frequency standards; antennas, rf systems, electromagnetic propagation phenomena, space communication systems.

Materials Sciences Laboratory: Development of new materials: metals, alloys, ceramics, polymers and their composites, and new forms of carbon; non-destructive evaluation, component failure analysis and reliability; fracture mechanics and stress corrosion; analysis and evaluation of materials at cryogenic and elevated temperatures as well as in space and enemy-induced environments.

Space Sciences Laboratory: Magnetospheric, auroral and cosmic ray physics, wave-particle interactions, magnetospheric plasma waves; atmospheric and ionospheric physics, density and composition of the upper atmosphere, remote sensing using atmospheric radiation; solar physics, infrared astronomy, infrared signature analysis; effects of solar activity, magnetic storms and nuclear explosions on the earth's atmosphere, ionosphere and magnetosphere; effects of electromagnetic and particulate radiations on space systems; space instrumentation.